DOI: 10.1002/ejic.200801162

Indenyl- and Fluorenyl-Functionalized N-Heterocyclic Carbene Complexes of Rhodium and Iridium – Synthetic, Structural and Catalytic Studies

Stephen P. Downing,[a] Peter J. Pogorzelec,[b] Andreas A. Danopoulos,*[a] and David J. Cole-Hamilton*[b]

Keywords: N-Heterocyclic carbenes / Carbenes / Carbene ligands / Rhodium / Iridium / Carbonylation / Cyclopentadienyl complexes

Rhodium and iridium complexes with N-heterocyclic carbenes (NHC) functionalized with neutral or anionic indenyl and fluorenyl groups are reported. In the complexes the ligands adopt monodentate, bidentate or bridging bonding modes with the NHC group σ-bonded and the fluorenyl or indenyl functionalities either dangling or coordinated to the metal with various hapticities (η^1, η^3 and η^5). Metallation of the C–H bond of the alkylene linker in the ligand has also been observed. Catalytic studies on the bidentate Rh^I complex **6** show that it is weakly active for the hydroformylation of 1-octene with poor linear selectivity, but it shows slightly lower activity than the standard Monsanto system for the carbonylation of methanol.

Introduction

Strongly σ-donating N-heterocyclic carbene (NHC) ligands have been used as phosphane replacements in the synthesis of late-transition-metal complexes, where an electron-rich metal centre with robust metal–ligand bond and a well-defined structure is desirable, especially for catalytic applications.[1] NHC complexes have proven to be useful catalysts in cross-coupling reactions of unreactive aryl halides,[2] telomerization reactions[3a] and metathesis[3b] but also in hydroformylation[4] where their advantages over the established phosphane complexes are less dramatic, mainly, due to competing unwanted alkene isomerization under the reaction conditions.

Methanol carbonylation to acetic acid is carried out on an industrial scale and is based on $[Rh(CO)_2I_2]^-$ and $[Ir(CO)_2I_2]^-$ catalysts, the latter promoted with ruthenium carbonyl complexes. Electron-rich Rh^I phosphane complexes have been targeted as high-activity methanol carbonylation catalysts, because they are expected to accelerate the rate-determining oxidative addition of the MeI to Rh^I. In a further development, cyclopentadienyl complexes of Co^I, Rh^I and Ir^I with tethered alkyl- and arylphosphanes have also been studied as catalysts for this reaction, and showed higher carbonylation rates under milder conditions.[5]

We have recently reported a new class of NHC ligands **Flu-NHC**, **Ind-NHC** and derivatives (Scheme 1), where the carbene is tethered, through a two- or three-carbon atom aliphatic linker, to indenyl or fluorenyl donor groups. We have also described their complexes with early transition metals.[6a,6b] The use of these ligands with lanthanides has been described by Wang.[6c] Tetramethylcyclopentadienyl analogues have also been reported recently.[7] The analogous cyclopentadienyls and indenyls with tethered phosphanes (**Ind-PPh$_2$** and **Cp^{Me4}-PEt$_2$** in Scheme 1) have been used in many cases for the synthesis of electron-rich, structurally rigid platinum-group metal complexes with catalytic potential.[5,8]

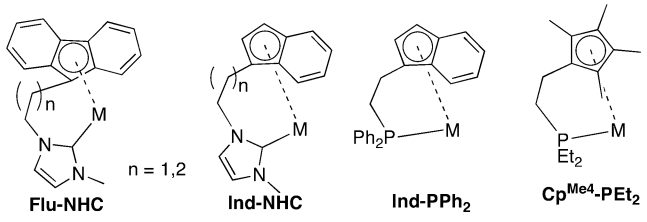

Scheme 1.

In this paper, we expand our studies with the **Flu-NHC** and **Ind-NHC** ligands to Rh^I and Ir^I. We also present possible limitations of the ligand design under certain coordination environments arising from competing reactivity involving C–H bonds of the ligand backbone. Lastly, we describe catalytic studies of one mononuclear chelate Rh^I carbonyl complex in hydroformylation of 1-octene and in the carbonylation of methanol and compare the activity in the latter with other known phosphane catalysts. The new complexes included in this paper and the transformations leading to them are shown in Schemes 2, 3, and 4.

[a] School of Chemistry, University of Southampton, Highfield, SO17 1BJ, UK
E-mail: ad1@soton.ac.uk
[b] EaStCHEM, School of Chemistry, University of St Andrews, Purdie Building, North Haugh, St Andrews, Fife, KY16 9ST, UK

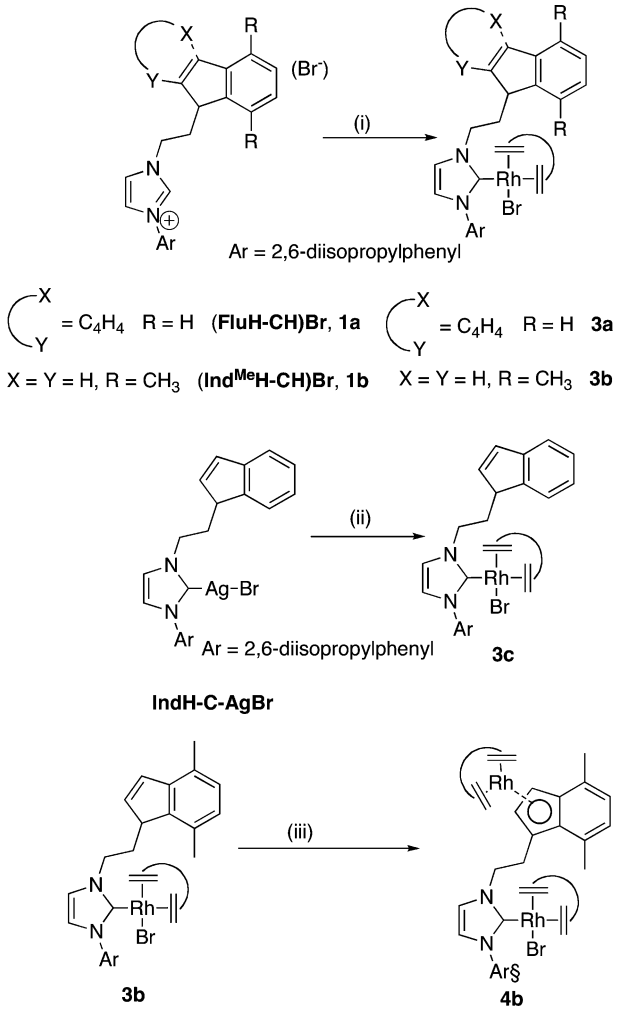

Scheme 2. The synthesis of Rh complexes with monodentate NHC ligands containing dangling fluorene/indene groups and with bridging NHC-dimethylindenyl ligands. Reagents: (i) 0.5 equiv. $[Rh(COD)(OMe)]_2$, THF; (ii) 0.5 equiv. $[Rh(COD)Cl]_2$, THF; (iii) 0.5 equiv. $[Rh(COD)(OMe)]_2$, toluene reflux.

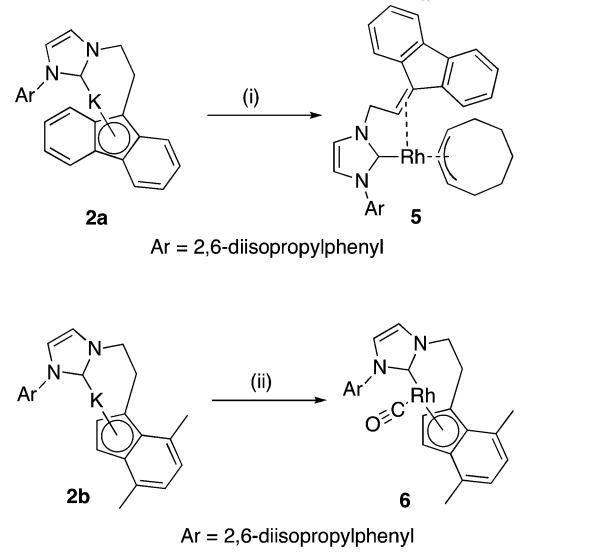

Scheme 3. Rh complexes with the η^2-fluorenyl-fulvene and the bidentate Ind^{Me}-NHC ligand. Reagents: (i) $[Rh(COD)Cl]_2$, (ii) $[Rh(CO)_2Cl]_2$.

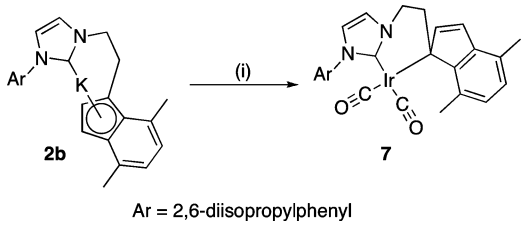

Scheme 4. The synthesis of Ir complexes. Reagents: (i) $[Ir(COD)Cl]_2$, CO, THF.

Results and Discussion

Rhodium Complexes: Rhodium NHC complexes have been prepared in the past by the "silver transmetallation" method[9a] or by deprotonation of imidazolium salts with bases in the presence of suitable Rh precursors[9b] or with bases coordinated to Rh (mainly in $[Rh(1,5\text{-COD})(OMe)]_2$).[9c] Reaction of the imidazolium salts (**FluH-NHCH**)Br **1a** or (**Ind^{Me}H-NHCH**)Br **1b** with $[Rh(1,5\text{-COD})(OMe)]_2$ gave good yields of the air-stable, yellow to red rhodium complexes **3a** and **3b** (see Scheme 2).

The new complexes were characterized by analytical, spectroscopic and single-crystal X-ray diffraction methods. Furthermore, reaction of the previously reported silver complexes Ag(**IndH-NHC**)Br and Ag(**Ind^{Me}H-NHC**)Br[6] with $[Rh(COD)Cl]_2$ gave **3b** and **3c**, respectively. The absence of a resonance due to the imidazolium proton in the ^{1}H NMR of **3a**–**3c** supports the formation of a Rh–C_{NHC} bond after deprotonation at the C2 of the imidazolium salt, however, the presence of peaks at ca. δ = 7.32 (**3a**) and δ = 6.10 ppm (**3b** and **3c**) indicated that the cyclopentadienyl-type ring was not deprotonated. The difference in the pK_a of the imidazolium salts and cyclopentadienyl moiety has been previously documented and is in agreement with the trends observed here.[6] Structural determination of **3a**, **3b** and **3c** (see Figures 1, 2 and 3, respectively) confirmed the ^{1}H NMR conclusions. Important bond lengths and angles are given in the captions of the Figures. In all three complexes, the metal adopts a square-planar geometry, with monodentate NHC ligand and dangling fluorene and indene aromatic rings. A bromide and a chelating 1,5-COD complete the coordination sphere in all three cases. The bond lengths are in the range previously reported for similar complexes.[10]

The availability of the dangling indene in **3b** and **3c** pointed to the possibility of a rational construction of bimetallic complexes by subsequent deprotonation of the indene followed by reaction with electrophilic metal precursors. Although deprotonation of **3b** and **3c** (for example by alkyllithium compounds) was evident, in most cases intractable mixtures were obtained after the addition of the metal electrophile. However, heating of solutions of **3b** in toluene with one-half equivalent of $[Rh(1,5\text{-COD})(OMe)]_2$ gave, after work up, the bimetallic complex **4b** in low yields. The disappearance of the peak at δ = 6.10 ppm in the ^{1}H NMR

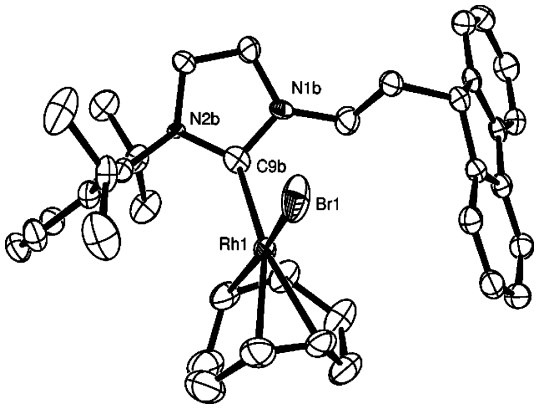

Figure 1. ORTEP representation of the molecular structure of **3a** showing 50% probability ellipsoids (see also experimental section). H atoms and disordered THF solvent are omitted for clarity. Selected bond lengths [Å] and angles [°] with estimated standard deviations in parentheses: C(1)–C(2) 1.374(8), C(5)–C(6) 1.370(8), C(1)–Rh(1) 2.095(5), C(2)–Rh(1) 2.120(5), C(5)–Rh(1) 2.178(5), C(6)–Rh(1) 2.221(5), C(9A)–N(2A) 1.4200 C(9A)–N(1A) 1.4200; C(9A)–Rh(1) 2.000(5), Br(1)–Rh(1) 2.5088(10), N(2A)–C(9A)–N(1A) 108.0; N(2A)–C(9A)–Rh(1) 125.1(4), N(1A)–C(9A)–Rh(1) 126.7(4), C(9A)–Rh(1)–C(1) 97.6(2), C(9A)–Rh(1)–C(9B) 12.69(18), C(1)–Rh(1)–C(9B) 85.1(2), C(9A)–Rh(1)–C(2) 99.3(2), C(1)–Rh(1)–C(2) 38.0(2), C(9B)–Rh(1)–C(2) 88.05(19), C(9A)–Rh(1)–C(5) 156.8(2), C(1)–Rh(1)–C(5) 97.4(2), C(9B)–Rh(1)–C(5) 159.9(2).

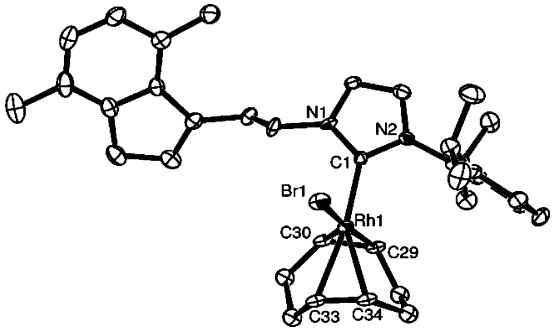

Figure 2. ORTEP representation of the molecular structure of **3b** showing 50% probability ellipsoids. H atoms are omitted for clarity. Selected bond lengths [Å] and angles [°] with estimated standard deviations in parentheses: C(1)–N(1) 1.337(11), C(1)–N(2) 1.366(12), C(1)–Rh(1) 2.025(9), C(29)–C(30) 1.460(14), C(33)–C(34) 1.362(15), C(29)–Rh(1) 2.149(10), C(30)–Rh(1) 2.102(10), C(33)–Rh(1) 2.236(10), C(34)–Rh(1) 2.176(9), Br(1)–Rh(1) 2.5018(12), N(1)–C(1)–N(2) 104.3(8), N(1)–C(1)–Rh(1) 128.4(7), N(2)–C(1)–Rh(1) 127.3(7), C(1)–Rh(1)–C(30) 92.0(4), C(1)–Rh(1)–C(29) 89.7(4), C(1)–Rh(1)–C(34) 153.6(4), C(30)–Rh(1)–C(34) 98.3(4), C(29)–Rh(1)–C(34) 82.9(4), C(1)–Rh(1)–C(33) 170.0(4), C(30)–Rh(1)–C(33) 81.2(4), C(29)–Rh(1)–C(33) 89.7(4), C(1)–Rh(1)–Br(1) 90.3(3), C(30)–Rh(1)–Br(1) 147.6(3), C(29)–Rh(1)–Br(1) 172.3(3), C(34)–Rh(1)–Br(1) 93.7(3), C(33)–Rh(1)–Br(1) 91.6(3)..

spectrum is diagnostic of the deprotonation of the indene ring. The molecular structure of **4b** was established crystallographically and is shown in Figure 4. Important bond lengths and angles are included in the caption of Figure 4. The molecule contains two Rh centres with different coordination spheres. The first centre (crystallographic Rh1) is square planar and coordinated to 1,5-COD, one bromide

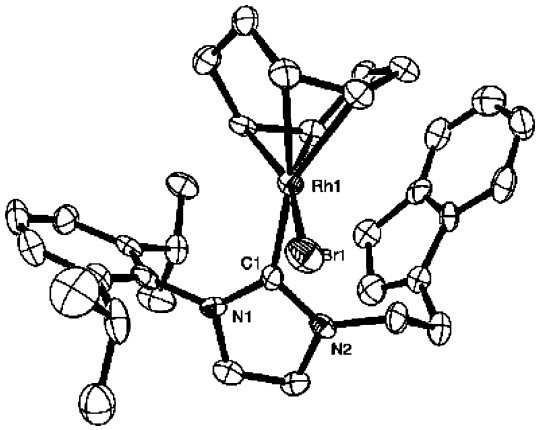

Figure 3. ORTEP representation of the molecular structure of **3c** showing 50% probability ellipsoids. H atoms are omitted for clarity. Selected bond lengths [Å] and angles [°] with estimated standard deviations in parentheses: Rh(1)–C(1) 2.041(9), Rh(1)–C(32) 2.098(9), Rh(1)–C(31) 2.124(8), Rh(1)–C(28) 2.170(9), Rh(1)–C(27) 2.210(10), Rh(1)–Br(1) 2.5069(13), N(2)–C(1) 1.367(11), N(1)–C(1) 1.369(10), C(27)–C(28) 1.382(14), C(31)–C(32) 1.386(12), C(1)–Rh(1)–C(32) 93.8(3), C(1)–Rh(1)–C(31) 93.4(3), C(1)–Rh(1)–C(28) 155.6(4), C(32)–Rh(1)–C(28) 96.9(4), C(31)–Rh(1)–C(28) 81.7(4), C(1)–Rh(1)–C(27) 167.6(4), C(32)–Rh(1)–C(27) 81.3(4), C(31)–Rh(1)–C(27) 89.7(4), C(1)–Rh(1)–Br(1) 88.3(2), C(32)–Rh(1)–Br(1) 158.8(3), C(31)–Rh(1)–Br(1) 162.6(3), C(28)–Rh(1)–Br(1) 89.6(3), C(27)–Rh(1)–Br(1) 92.3(3).

and one NHC. The second (crystallographic Rh2) is bound to an indenyl and 1,5-COD. All five Rh2–$C_{indenyl}$ distances lie in the range 2.218(6) – 2.360(8) Å. The Rh – C_{NHC} distance [2.030(6) Å] falls within the range reported in the literature for similar bonds.[10] The Rh1–C_{COD} distances on the average are longer than Rh2–C_{COD} reflecting the higher *trans* influence of the NHC ligand. Multimetallic complexes with NHC ligands have recently been reported and may exhibit metal cooperativity in certain catalytic reactions.[11] The catalytic properties of **4b** have not been studied.

Because one of our initial aims was to synthesize complexes in which both the anionic cyclopentadienyl and the NHC functionalities were chelating to the same Rh centre and compare their catalytic properties with the known phosphane analogues, we treated $[Rh(COD)Cl]_2$ with one half equivalent of (**Flu-NHC**)$^-K^+$ **2a** (Scheme 3).[6]

In this case an unexpected C–H activation took place leading to low yields of **5**; persistent contamination by other unidentified Rh complexes inhibited full spectroscopic and analytical characterization of **5**; however its structure was determined crystallographically (see Figure 5); important bond lengths and angles are given in the caption of the Figure. The complex contains a Rh centre with a distorted square-planar geometry due to ligand-imposed constraints. In addition to the NHC donor, there are one η^3-cyclooctenyl group and one severely distorted η^2-alkene type bonding involving the fluorenyl C9 and its neighbouring C atom of the linker, resulting in a η^2-coordinated substituted fulvene. Even though the Rh–C_{NHC} bond length is not unusual [2.017(3) Å] there is a severe distortion of the NHC bonding as evidenced by the two angles N2–C1–Rh1 140.9°

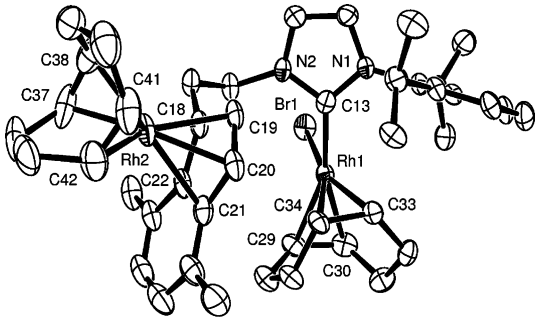

Figure 4. ORTEP representation of the molecular structure of **4b** showing 50% probability ellipsoids. H atoms are omitted for clarity. Selected bond lengths [Å] and angles [°] with estimated standard deviations in parentheses: C(13)–Rh(1) 2.030(6), C(13)–N(1) 1.372(7), C(13)–N(2) 1.365(7), Br(1)–Rh(1) 2.5051(10), C(29)–Rh(1) 2.196(6), C(30)–Rh(1) 2.210(7), C(33)–Rh(1) 2.111(6), C(34)–Rh(1) 2.120(6), C(29)–C(30) 1.373(9), C(33)–C(34) 1.417(8), C(18)–Rh(2) 2.220(6), C(19)–Rh(2) 2.235(6), C(20)–Rh(2) 2.218(6), C(21)–Rh(2) 2.357(7), C(22)–Rh(2) 2.360(6), C(37)–Rh(2) 2.110(7), C(38)–Rh(2) 2.138(8), C(41)–Rh(2) 2.127(7), C(42)–Rh(2) 2.126(7), C(37)–C(38) 1.398(12), C(41)–C(42) 1.377(11), N(2)–C(13)–N(1) 103.0(5), N(2)–C(13)–Rh(1) 123.0(4), N(1)–C(13)–Rh(1) 133.0(4), (13)–Rh(1)–Br(1) 86.96(16).

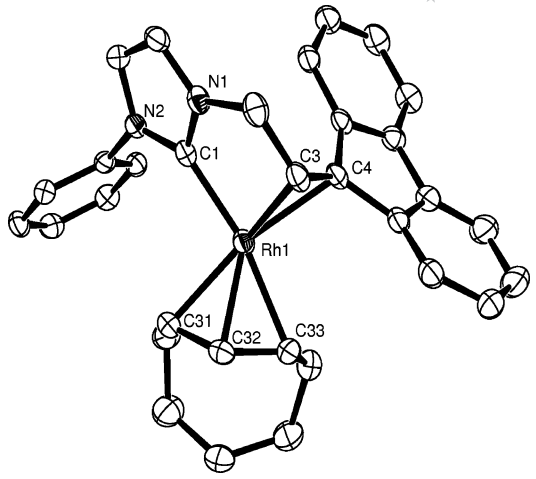

Figure 5. ORTEP representation of the molecular structure of **5** showing 50% probability ellipsoids. H atoms and *i*Pr groups are omitted for clarity. Selected bond lengths [Å] and angles [°] with estimated standard deviations in parentheses: Rh(1)–C(1) 2.017(3), Rh(1)–C(3) 2.082(3), Rh(1)–C(4) 2.238(2), Rh(1)–C(31) 2.179(3), Rh(1)–C(32) 2.125(3), Rh(1)–C(33) 2.214(3), C(1)–Rh(1)–C(3) 80.66 (10), C(1)–Rh(1)–C(4) 92.10 (10), C1–Rh(1)–C(32) 130.79 (10), N(1)–C(1)–N(2) 130.4(2).

and N1–C1–Rh1 115.6°. The distortion in the Rh–η^2-fulvene bonding (Rh1–C3 2.082 Å and Rh1–C4 2.238 Å) is possibly due to steric reasons. There are only very few examples of structurally characterized η^2-fulvene type fluorene complexes (Ru, Fe) and in the known cases the η^2-bonding asymmetry is less severe or does not exist at all.[12] It could be envisaged that **5** is obtained by a sequence of metallation of the fluorenyl C-9 to form an η^1-fluorenyl complex, followed by β-H elimination from the α-CH_2 of the ethylene linker and subsequent conversion of the η^4-cyclooctadiene hydride to the η^3-cyclooctenyl ligand. The initiation of this sequence, which involves oxidative addition of a C–H bond, may be favoured by the high metal basicity due to the presence of σ-donating NHC in combination with the absence of strong π-acceptor co-ligands (e.g. CO). The scope of application of these types of ligands in catalysis may therefore be limited (see also below).

Reaction of **2b** with $[Rh(CO)_2Cl]_2$ gave good yields of the complex **6**; no products due to metallation of ligand C–H bonds were observed. Complex **6** was characterized by spectroscopic, analytical and diffraction methods. Interestingly, the metal π-basicity in **6** can be compared to that in Rh(**Cp^{Me4}-PEt$_2$**)(CO),[5,8] and Rh(**Ind-PPh$_2$**)(CO)[8] by the degree of backbonding to the coordinated CO as measured from the position of the ν(CO) in the IR spectra of the complexes. The ν(CO) of **6** appears at slightly lower wave numbers (1927 cm^{-1}) than those for the phosphane species (1933 and 1937 cm^{-1} for PEt_2 and PPh_2 analogues, respectively). This small shift should be interpreted with care due to the different electronic features of the cyclopentadienyl co-ligands, which may also influence the electron density on the metal, but it does suggest very high electron density on the metal. The structure of **6** is shown in Figure 6; important bond lengths and angles are given in the caption of the Figure. The Rh has adopted a distorted square-planar geometry with one indenyl ligand, one NHC and one CO donors. The Rh–$C_{indenyl}$ bonds span the range 2.210–2.388 Å. The Rh – C10 [2.388(4) Å] and Rh – C11 [2.383(4) Å] are longer than the sum of covalent radii of Rh and C and therefore the bonding interaction between the atoms is weak or non-existent. In the latter case, the indenyl ring is "slipped" with a η^3-allyl type coordination, rendering the Rh centre 16-electron species. It is not surprising that this distortion cannot be detected in solution by NMR spectroscopy. Comparable discrepancy in the Rh–$C_{indenyl}$ distances has been observed in Rh(**Ind-PPh$_2$**)CO but the authors proposed a η^5-structure in this case.[8] The Rh–

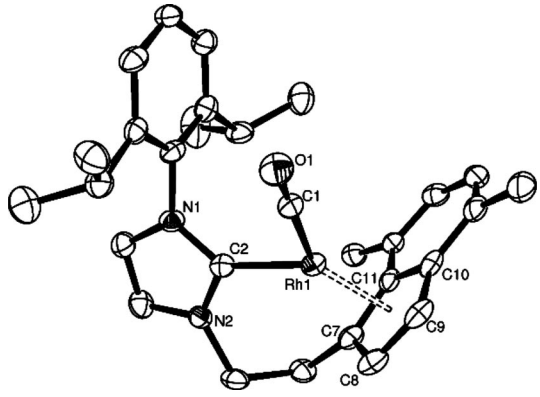

Figure 6. ORTEP representation of the molecular structure of **6** showing 50% probability ellipsoids. H atoms are omitted for clarity. Selected bond lengths [Å] and angles [°] with estimated standard deviations in parentheses: C(1)–O(1) 1.157(4), C(1)–Rh(1) 1.833(4), C(2)–N(2) 1.368(5), C(2)–N(1) 1.372(5), C(2)–Rh(1) 1.990(4), C(7)–Rh(1) 2.210(4), C(8)–Rh(1) 2.251(4), C(9)–Rh(1) 2.261(4), C(10)–Rh(1) 2.388(4), C(11)–Rh(1) 2.383(4), O(1)–C(1)–Rh(1) 175.7(4), N(2)–C(2)–N(1) 103.2(3), N(2)–C(2)–Rh(1) 123.3(3), N(1)–C(2)–Rh(1) 133.5(3), C(1)–Rh(1)–C(2) 96.64(15).

C_{NHC} bond length [1.990(4) Å] is unremarkable. The plane of the heterocyclic imidazole ring lies 2.6° from the Rh–C_{NHC} vector. The Rh–C_{CO} [1.833(4) Å] and C–O [1.157(4) Å] distances are not significantly different (within the measured esds) than those in the analogous Rh(**Ind-PPh$_2$**)(CO) and Rh(**Cp^{Me4}-PEt$_2$**)(CO). The relative degree of donation by the PEt_2 and $CpMe_4$ donors in comparison to NHC and indenyl or competing backbonding between NHC and CO ligands is not clear.

Iridium Complexes: Initial attempts to extend the above chemistry to iridium involved the reaction of $[Ir(COD)Cl]_2$ with the potassium salts **2b** or **2c**[6a] (Scheme 4). This reaction gave complicated mixtures of products from which a few complexes with metallated ligand backbones were characterized crystallographically but could not be isolated as analytically pure samples. However, the reaction of $[Ir(COD)Cl]_2$ with the potassium complex **2b** under CO gave good yields of complex **7** which was characterized by spectroscopic and crystallographic methods.

The structure of **7** is shown in Figure 7; important bond lengths and angles are given in the caption of the Figure. The complex contains a square-planar iridium coordinated by two *cis*-CO and one chelate dimethyl indenyl-NHC ligands; the dimethylindenyl group is bonded through only one C atom (η^1). The two Ir–C_{CO} bond lengths are very similar [1.871(8) and 1.889(8) Å] the longer being *trans* to the NHC. The Ir–C_{NHC} [2.083(7) Å] and Ir–$C_{indenyl}$ [2.220(7) Å] are longer than similar bonds reported in the literature, which may be due to the strong *trans* influence of the CO *trans* to them.

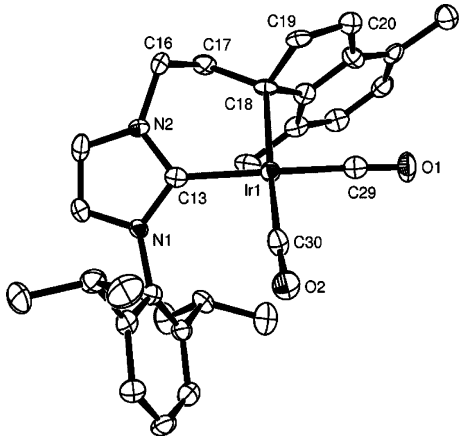

Figure 7. ORTEP representation of the molecular structure of **7** showing 50% probability ellipsoids. H atoms are omitted for clarity. Selected bond lengths [Å] and angles [°] with estimated standard deviations in parentheses: C(13)–N(2) 1.354(9), C(13)–N(1) 1.366(8), C(13)–Ir(1) 2.083(7), C(18)–Ir(1) 2.220(7), C(29)–O(1) 1.139(8), C(29)–Ir(1) 1.889(8), C(30)–O(2) 1.136(9), C(30)–Ir(1) 1.871(8), N(2)–C(13)–N(1) 104.2(6), N(2)–C(13)–Ir(1) 125.0(5), N(1)–C(13)–Ir(1) 130.5(5), C(19)–C(18)–C(26) 101.6(6), C(19)–C(18)–C(17) 109.9(6), C(26)–C(18)–C(17) 115.0(6), C(19)–C(18)–Ir(1) 101.5(4), C(26)–C(18)–Ir(1) 111.8(5), C(17)–C(18)–Ir(1) 115.2(5), C(30)–Ir(1)–C(29) 89.9(3), C(30)–Ir(1)–C(13) 92.4(3), C(29)–Ir(1)–C(13) 175.6(3), C(30)–Ir(1)–C(18) 174.5(3), C(29)–Ir(1)–C(18) 87.8(3), C(13)–Ir(1)–C(18) 90.2(3), O(1)–C(29)–Ir(1) 177.1(7), O(2)–C(30)–Ir(1) 175.0(7).

Catalytic Studies: Compound **6** was tested for its catalytic activity in the hydroformylation of 1-octene and especially in the carbonylation of methanol, because the related complexes containing dialkylphosphanylethylcyclopentadienyl ligands showed high activity and because **6** has also very high electron density on Rh as indicated by the low value of ν(CO). High electron density should accelerate the reaction with methyl iodide, which is often rate determining, although too high an electron density can slow reductive elimination of MeC(O)I to such a level that it becomes rate determining and gives a lower overall reaction rate, as is observed for Rh(**Cp$^{Me}_4$-PEt$_2$**)(CO). Complex **6** showed some activity for the hydroformylation of 1-octene (Scheme 5) with slow gas uptake being observed over 8 h. Product analysis shows that extensive alkene isomerisation competes with hydroformylation and that the isomerized alkenes are also hydroformylated, as indicated by the presence of significant amounts of 2-ethylheptanal and 2-propylhexanal in addition to 2-methyloctanal and nonanal. The overall linear/branched aldehyde ratio is only 1.25.

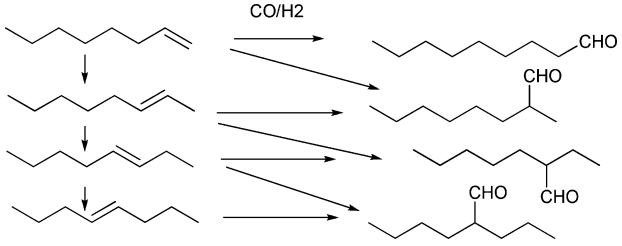

Scheme 5. Products obtained during the hydroformylation of 1-octene catalysed by **6**. All the compounds shown are observed in the product mixture.

Methanol carbonylation (Scheme 6) using **6** was more successful. The results of reactions carried out at 120, 150 and 180 °C are shown in Table 1, where they are compared with the standard Monsanto system (catalyst $[RhI_2(CO)_2]^-$), [Rh(**Cp^{Me4}-PPh$_2$**)(CO)], the most active catalyst of its class and [Rh(**Cp^{Me4}-PEt$_2$**)(CO)], the one with the highest electron density.[8] The results reported in ref.[8] were obtained with a catalyst loading 0.25 times that used in this study. The comparative rates reported in this paper when using [Rh(**Cp^{Me4}-PEt$_2$**)(CO)] and $[RhI_2(CO)_2]^-$ were obtained at the same catalyst loading as that used for **6** (5×10^{-3} mol dm^{-3}), whilst the rate for [Rh(**Cp^{Me4}-PPh$_2$**)(CO)] was extrapolated from published data[8a] assuming a first order dependence on [Rh]. This assumption was approximately valid for [Rh(**Cp^{Me4}-PEt$_2$**)(CO)] and for $[RhI_2(CO)_2]^-$.

The reactions were monitored keeping the pressure in the autoclave constant at 27 bar, by feeding CO from a ballast vessel. For **6** at all temperatures, these gas uptake plots were linear until the substrate was close to exhaustion, showing that the reaction is zero order in substrate, as is usual for these reactions, but also that the catalyst was stable under these reaction conditions. Decomposition during the runs usually leads to non-linear gas uptake curves. Compound **6** proved to be slightly less active than the Monsanto system

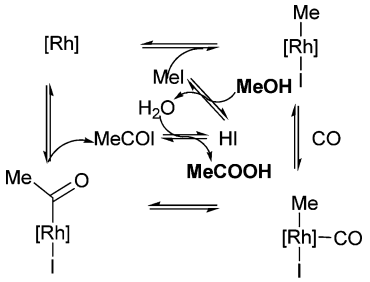

Scheme 6. General mechanism for the carbonylation of methanol in the presence of MeI catalysed by rhodium complexes.

Table 1. Catalytic data for the carbonylation of methanol.[a]

Catalyst	T [°C]	Rate [mol dm^{-3}h^{-1}]	Reference
6	120	0.39	this work
6	150	1.5	this work
6	180	3.9	this work
$[RhI_2(CO)_2]^-$	150	1.7	this work
[Rh(Cp^{Me4}-PEt$_2$)(CO)]	150	1.5	this work
[Rh(Cp^{Me4}-PPh$_2$)(CO)]	150	3.2	extrapolated[b]

[a] For conditions, see Exp. Sect., [Rh] = 5×10^{-3} mol dm^{-3}. [b] See ref.[8a].

but comparable with [Rh(**CpMe$_4$-PEt$_2$**)(CO)] at 150 °C, suggesting that the very high electron density on rhodium may, as with [Rh(**CpMe$_4$-PEt$_2$**)(CO)], make reductive elimination of MeC(O)I slower than oxidative addition of MeI and hence rate determining. Importantly, the phosphane ligands are susceptible to reaction with MeI (added as a promoter) or give phosphane oxides, but such reactivity is not possible for the carbene complexes, which could account for the apparent stability of **6** even at high temperatures and provide a potential advantage in their use if their activity can be tuned electronically.

Conclusions

Compound **6**, containing the indenyl-functionalized heterocyclic carbene ligand bound through both moieties shows slightly lower activity for methanol carbonylation than the standard Monsanto catalyst, $[RhI_2(CO)_2]^-$, but about the same as that of the highly electron-rich [Rh(**Cp^{Me4}-PEt$_2$**)(CO)], suggesting that reductive elimination of acetyl iodide may be rate determining. Interestingly, it appears to be stable under the reaction conditions, which may point to possible optimization by electronic tuning. The application of the **Flu-NHC** and **Ind-NHC** ligands to the design of catalysts for other catalytic applications is an area of interest even though the metal basicity may interfere with ligand decomposition through metallation of the ligand backbone. The choice of co-ligands in this case may be important to provide functional complexes.

Experimental Section

General: Elemental analyses were carried out by the London Metropolitan University microanalytical laboratory. All manipulations were performed under nitrogen in a Braun glove box or using standard Schlenk techniques, unless stated otherwise. Solvents were dried using standard methods and distilled under nitrogen prior to use. The light petroleum used throughout had a boiling range of 40–60 °C. The starting materials (FluH-NHCH)Br, (IndH-NHCH)-Br, (Ind^{Me}H-NHCH)Br, IndH^{Me}-NHC-AgBr, (Flu-NHC)K, (Ind^{Me}-NHC)K,[6] [Rh(1,5-COD)Cl]$_2$,[13a] [Rh(1,5-COD)(OMe)]$_2$,[13b] [Ir(1,5-COD)Cl]$_2$[13a] were prepared according to literature procedures. All other chemicals were from commercial sources. NMR spectroscopic data were recorded with Bruker AV-300 and DPX-400 spectrometers, operating at 300 and 400 MHz (^{1}H), respectively. The spectra were referenced internally using the signal from the residual protio-solvent (^{1}H) or the signals of the solvent (^{13}C).

Synthesis of Complex 3a: [Rh(COD)(OMe)]$_2$ (0.5 mmol, 240 mg) and the (FluH-NHCH)Br (1.0 mmol, 500 mg) were dissolved in THF (20 mL) and cooled to –78 °C. The solutions were combined. The reaction mixture was warmed to room temperature and stirred overnight. The volatiles were removed under reduced pressure. The residue was dissolved in the minimum of THF (5 mL) which was then layered with ether. The product was isolated as X-ray quality crystals by filtration. Drying gave the product as a yellow crystalline material (70%, 490 mg). ^{1}H NMR (C_6D_6, 300 MHz): δ = 7.98–7.90 (m, 4 H, Ar), 7.80 (d, J = 6 Hz, 1 H, Ar), 7.58 (dd, J = 7.2 Hz, 1 H, Ar), 7.52–7.35 (m, 5 H, Ar), 7.32 (dd, J = 7.1 Hz, 1 H, Ar), 7.23 (d, J = 7 Hz, 1 H, Ar), 5.08–4.90 (m, 1 H, COD-CH), 4.72–4.38 (m, 3 H, COD-CH × 3), 4.23 (t, J = 6 Hz, 1 H, bridge), 3.60–3.35 (m, 1 H, bridge), 3.18–2.90 [m, 2 H, CH(CH$_3$)$_2$], 2.84–2.62 (m, 1 H, bridge), 2.30–2.22 (m, 1 H, bridge), 1.80–1.42 (m, 2 H, COD-CH$_2$ × 2), 1.80–1.72 (m, 3 H, COD-CH$_2$ × 3), 1.72–1.42 (m, 2 H, COD-CH × 2), 1.42–1.32 [m, 3 H, CH(CH$_3$)$_2$], 1.30–1.12 (m, 1 H, COD-CH$_2$), 1.10–0.85 [m, 9 H, CH(CH$_3$)$_2$] ppm. ^{13}C{^{1}H}NMR (C_6D_6, 100 MHz): δ = 146.6 (Ar), 146.4 (Ar), 146.0 (Ar), 145.3 (Ar), 140.5 (Ar), 135.4 (Ar), 129.5 (ArH), 127.2 (ArH), 127.1 (ArH), 126.9 (ArH), 125.7 (ArH), 125.5 (ArH), 125.4 (ArH), 124.4 (ArH), 123.9 (ArH), 123.1 (ArH), 121.0 (ArH), 120.0 (ArH), 49.1 (CH$_2$), 45.2 (Fluorenyl-C), 40.0 (CH$_2$), 33.7 (CH$_2$), 33.2 (CH$_2$), 30.6 (CH$_2$), 30.2 (CH$_2$), 29.2 (CH), 27.6 (CH$_2$), 27.0 (CH), 26.0 (CH), 25.5 (CH), 25.1 [CH(CH$_3$)$_2$], 23.7 [CH(CH$_3$)$_2$], 23.4 [CH(CH$_3$)$_2$], 22.4 [CH(CH$_3$)$_2$] ppm. MS (ES$^+$): m/z = 630 [M – Br$^-$]. $C_{38}H_{44}BrN_2Rh{\cdot}C_4H_8O$: calcd. C 64.24, H 6.10, N 3.94; found C 64.61 H, 5.80, N 4.01.

Crystal data: CCDC-710639 (for **3a**), empirical formula $C_{38}H_{44}BrN_2Rh{\cdot}C_4H_8O$, formula weight 783.68, crystal system triclinic, space group $P\bar{1}$, a = 10.313(5) Å b = 13.442(5) Å, c = 15.119(5) Å, α = 68.598(5)°, β = 70.798(5)°, γ = 86.647(5)°, V = 1838.3(13) Å^3, Z = 2, T = 120(2), μ = 1.586 mm^{-1}, data collected 34024, unique data 8420, goodness of fit on F^2 = 1.033, $R_{int.}$ =0.0471, final $R(|F|)$ for $F_o > 2\sigma(F_o)$ = 0.0627, final $R(F^2)$ for all data 0.1458.

Synthesis of Complex 3b: Prepared as above from [Rh(COD)-(OMe)]$_2$ and (Ind^{Me}H-NHCH)Br; yield 72%. ^{1}H NMR (C_6D_6, 300 MHz): δ = 7.34 (d, J = 8 Hz, 1 H, Ar), 7.28 (dd, J = 8.2 Hz, 1 H, Ar), 7.07 (dd, J = 8.2 Hz, 1 H, Ar), 6.91 (d, J = 7 Hz, 1 H, Ar), 6.87 (d, J = 2 Hz, 1 H, NCH), 6.83 (d, J = 7 Hz, 1 H, Ar), 6.70 (d, J = 2 Hz, 1 H, NHC), 6.09 (s, 1 H, indene-H), 5.61–5.50 (m, 1 H, bridge), 4.90–4.80 (m, 1 H, COD), 4.78–4.69 (m, 1 H, COD), 4.55–4.45 (m, 1 H, bridge), 3.60–3.26 [m, 4 H, COD and CH(CH$_3$)$_2$], 3.25 (s, 3 H, indenyl-methyl), 3.20–3.09 (m, 1 H, bridge), 2.90–2.80 (m, 1 H, bridge), 2.60 (s, 3 H, indene-methyl), 1.90–1.70 (m, 5 H, COD), 1.60–1.20 (m, 3 H, COD), 1.39 [d, J = 7 Hz, 3 H, CH(CH$_3$)$_2$], 1.02 [d, J = 7 Hz, 3 H, CH(CH$_3$)$_2$], 1.01 [d,

J = 7 Hz, 3 H, $CH(CH_3)_2$], 0.86 [d, J = 7 Hz, 3 H, $CH(CH_3)_2$] ppm. $^{13}C\{^1H\}$ NMR: δ = (C_6D_6, 75 MHz): 146.9 (Ar), 144.4 (Ar), 142.5 (Ar), 141.3 (Ar), 140.7 (Ar), 134.8 (Ar), 129.7 (ArH), 128.7 (Ar), 128.6 (ArH), 127.1 (ArH), 125.2 (ArH), 123.8 (ArH), 123.6 (ArH), 122.1 (ArH), 119.3 (ArH), 95.6 (CH), 95.5 (CH), 95.4 (CH), 68.0 (CH_2), 67.6 (CH_2), 66.9 (CH_2), 50.9 (CH_2), 35.4 (CH_2), 32.3 (CH_2), 30.7 (CH_2), 30.4; (CH_2), 28.1 (CH), 27.7 (CH), 27.4 (CH), 27.3 (CH), 27.2 (CH), 24.8 (CH_2), 24.6 (CH), 23.2 (CH), 22.9 (CH), 27.8 (CH), 19.1 (CH), 17.3 (CH) ppm. $C_{36}H_{46}BrN_2Rh$ (689.58): calcd. C 62.61, H 6.86, N 4.06; found C 62.60, H 6.59, N 3.95.

Crystal data: CCDC-710640 (for **3b**), empirical formula $C_{36}H_{46}BrN_2Rh$, formula weight 689.58, crystal system triclinic, space group $P\bar{1}$, a = 8.2436(2) Å b = 8.5687(3) Å c = 22.8614(8) Å, α = 81.819(2)° β = 85.004(2)° γ = 82.286(2)° V = 1580.15(9) Å^3 Z = 2, T = 120(2) μ = 1.832, data collected 32381, unique data 7288, goodness of fit on F^2 = 1.171, $R_{int.}$ = 0.0647, final $R(|F|)$ for $F_o > 2\sigma(F_o)$ = 0.0955, final $R(F^2)$ for all data 0.2427.

Synthesis of Complex 3c: IndH^{Me}-NHC-AgBr (1.0 mmol, 560 mg) and $[Rh(COD)Cl]_2$ (0.5 mmol, 250 mg) were dissolved in toluene (10 mL) and heated to reflux for 18 h, the resulting solution was filtered through Celite and the solvents evaporated to dryness to give the crude product. Crystallization took place from toluene (10 mL) layered with petroleum ether (50%, 310 mg). ^1H NMR (C_6D_6, 400 MHz): δ = 7.48 (d, J = 8 Hz, 1 H, Ar), 7.36 (t, J = 8 Hz, 1 H, Ar), 7.27 (dd, Ar, J = 8.2 Hz, 1 H), 7.24 (t, J = 8 Hz, 1 H, Ar), 7.18–7.10 (m, 2 H, Ar), 7.07 (dd, J = 8.2 Hz, 1 H, Ar), 6.87 (d, J = 2 Hz, 1 H, NCH), 6.67 (d, J = 2 Hz, 1 H, NCH), 6.12 (s, 1 H, indene-H), 5.54–5.47 (m, 1 H, indene-H), 4.77–4.72 (m, 1 H, indene-H), 4.68–4.64 (m, 1 H, bridge), 4.53–4.46 (m, 1 H, bridge), 3.40 [sept, J = 7 Hz, 1 H, $CH(CH_3)_2$], 3.23 [sept, J = 7 Hz, 1 H, $CH(CH_3)_2$], 3.10–3.06 (m, 1 H, bridge), 2.74–2.72 (m, 1 H, bridge), 2.01–1.96 (m, 4 H, COD-CH ×4), 1.61–1.38 (m, 5 H, COD-CH_2 ×5), 1.36–1.28 (m, 3 H, COD-CH_2 ×3), 1.42 [d, J = 7 Hz, 3 H, $CH(CH_3)_2$], 1.00 [d, J = 7 Hz, 3 H, $CH(CH_3)_2$], 0.98 [d, J = 7 Hz, 3 H, $CH(CH_3)_2$], 0.86 [d, J = 7 Hz, 3 H, $CH(CH_3)_2$] ppm. $^{13}C\{^1H\}$ NMR (C_6D_6, 100 MHz): δ = 146.9 (Ar), 144.3 (Ar), 143.7 (Ar), 143.2 (Ar), 129.2 (ArH), 128.7 (ArH), 125.3 (Ar), 123.9 (ArH), 123.5 (ArH), 122.9 (ArH), 121.9 (ArH), 119.3 (ArH), 118.0 (ArH), 95.9 (indene-CH), 66.9 (COD), 66.8 (indene-C), 66.7 (CH_2), 49.8 (CH_2), 36.9 (CH_2), 32.6 (CH_2), 30.6 (CH_2), 30.5 (CH), 29.9 (CH_2), 28.3 (CH_2), 27.8 (CH), 27.3 (CH), 27.1 (CH_2), 27.0 [$CH(CH_3)_2$], 25.4 [$CH(CH_3)_2$], 24.9 [$CH(CH_3)_2$], 22.6 [$CH(CH_3)_2$] ppm. MS (ES^+): m/z = 581 [M – Br^-]. Accurate MS (ES^+): Calculated 581.2385; found 581.2385. $C_{34}H_{42}BrN_2Rh$: calcd. C 66.18, H 6.86, N 4.54; found C 66.12 H, 6.91, N 4.56.

Crystal data: CCDC-710641 (for **3c**), empirical formula $C_{34}H_{42}BrN_2Rh$, formula weight 661.52, crystal system orthorhombic, space group $P2_12_12_1$, a = 11.795(4) Å, b = 11.853(3) Å, c = 21.599(5) Å, α = 90°, β = 90°, γ = 90°, V = 3019.7(15) Å^3, Z = 4, T = 120(2) K, μ = 1.914 mm^{-1}, data collected 17562, unique data 6733, goodness of fit on F^2 = 0.973, $R_{int.}$ = 0.1500, final $R(|F|)$ for $F_o > 2\sigma(F_o)$ 0.0783, final $R(F^2)$ for all data 0.1520.

Synthesis of Complex 4b: Complex **3b** (0.5 mmol) and $[Rh(COD)(OMe)]_2$ (0.25 mmol) were dissolved in toluene (20 mL) and heated to reflux overnight. After cooling the toluene was removed under vacuum and the residues dissolved in THF (10 mL). After filtering the THF was layered with ether to give crystals of **4b**. ^1H NMR ([D_8]THF, 300 MHz): δ = 7.38 (d, 1 H, Ar), 7.25 (dd, J = 8.2 Hz, 1 H, Ar), 7.10 (dd, 1 H, Ar), 6.91 (d, J = 7 Hz, 1 H, Ar), 6.85 (d, J = 2 Hz, 1 H, NHC), 6.83 (d, J = 7 Hz, 1 H, Ar), 6.72 (d, 1 H, NHC), 5.65–5.50 (m broad, 2 H, bridge), 4.90–4.80 (m, 2 H, COD), 4.78–4.69 (m, 2 H, COD), 4.60–4.45 (m, 2 H, broad, bridge), 3.60–3.26 [m, 10 H, COD and $CH(CH_3)_2$], 3.20 (s, 3 H, indenyl-methyl), 2.90–2.75 (m, 2 H, broad bridge), 2.60 (s, 3 H, indene-methyl), 1.95–1.65 (m, 8 H, COD), 1.60–1.20 (m, 4 H, COD), 1.40 [d, 3 H, $CH(CH_3)_2$], 1.00 [d, 3 H, $CH(CH_3)_2$], 0.95 [d, J = 7 Hz, 3 H, $CH(CH_3)_2$], 0.85 [d, J = 7 Hz, 3 H, $CH(CH_3)_2$] ppm.

Crystal data: CCDC-710642 (for **4b**), empirical formula $C_{44}H_{57}BrN_2Rh_2$, formula weight 899.65, crystal system monoclinic, space group $P2_1/n$, a = 15.539(3) Å, b = 26.596(5) Å, c = 20.236(4) Å, α = 90°, β = 111.73(3)°, γ = 90°, V = 7769(3) Å^3, Z = 8, T = 120(2) K, μ = 1.911 mm^{-1}, data collected 63459, unique data 16317, goodness of fit on F^2 = 1.029, $R_{int.}$ = 0.0699, final $R(|F|)$ for $F_o > 2\sigma(F_o)$ = 0.0514, final $R(F^2)$ for all data 0.1470.

Formation of Complex 5: $[Rh(COD)(Cl)]_2$ (0.25 mmol, 120 mg) and the (**Flu-NHC**)$^-K^+$ (0.5 mmol, 230 mg) were combined as solids and precooled (–78 °C) THF (20 mL) was added at –78 °C. The mixture was allowed to reach room temperature slowly (ca. 2 h) and the solution was concentrated, filtered and layered with ether to give yellow crystals of **5** in low yield (ca. 20 mg). Analytically pure samples could not be obtained due to contamination with other rhodium-containing unidentifiable products.

Crystal data: CCDC-710643 (for **5**), empirical formula $C_{38}H_{43}N_2Rh$, formula weight 630.65, crystal system triclinic, space group $P\bar{1}$, a = 9.5366(5) Å, b = 10.3587(5) Å, c = 17.5823(9) Å, α = 82.455(2)°, β = 88.949(2)°, γ = 63.153(2)°, V = 1534.62(13) Å^3, Z = 2, T = 120(2) K, μ = 0.586 mm^{-1}, data collected 46366, unique data 7053, goodness of fit on F^2 = 1.028, $R_{int.}$ = 0.0683, final $R(|F|)$ for $F_o > 2\sigma(F_o)$ = 0.0392, final $R(F^2)$ for all data 0.0833.

Synthesis of Complex 6: $[Rh(CO)_2Cl]_2$ (0.5 mmol, 190 mg) and (**Ind^{Me}-NHC**)$^-K^+$ (1.0 mmol, 440 mg) were dissolved in THF (20 mL) and cooled to –78 °C. The two solutions were combined. The reaction mixture was warmed to room temperature and stirred overnight. The volatiles were removed under reduced pressure. The residue was dissolved in toluene (10 mL) and filtered through Celite. The toluene solution was layered with diethyl ether. X-ray-quality crystals formed and were isolated by filtration (80%, 424 mg). ^1H NMR (C_6D_6, 400 MHz): δ = 7.41 (m, 4 H, Ar), 7.08 (d, J = 7 Hz, 1 H, Ar), 6.81–6.74 (m, 1 H, Ar), 6.49 (d, J = 2 Hz, 1 H, NCH), 6.28 (d, J = 2 Hz, 1 H, NCH), 4.92–4.80 (m, 1 H, bridge), 3.60–3.50 (m, 1 H, bridge), 3.50–3.40 (m, 1 H, bridge), 3.20–3.12 (m, 1 H, bridge), 2.50 (s, 3 H, indene-CH_3), 2.25 (s, 3 H, indene-CH_3), 2.32–2.18 [m, 2 H, $CH(CH_3)_2$], 1.44 [d, J = 7 Hz, 6 H, $CH(CH_3)_2$], 1.09 [d, J = 7 Hz, 6 H, $CH(CH_3)_2$] ppm. $^{13}C\{^1H\}$ NMR (C_6D_6, 100 MHz): δ = 145.6 (Ar), 141.8 (Ar), 129.1 (Ar), 128.7 (Ar), 128.1 (ArH), 127.3 (ArH), 124.8 (ArH), 124.4 (Ar), 122.3 (Ar), 122.0 (Ar), 118.9 (ArH), 57.3 (CH_2), 49.4 (CH_2), 35.2 (indenyl-CH_3), 30.4 (indenyl-CH_3), 28.0 [$CH(CH_3)_2$], 27.1 [$CH(CH_3)_2$], 25.2 [$CH(CH_3)_2$], 21.7 [$CH(CH_3)_2$], 18.7 [$CH(CH_3)_2$], 16.9 [$CH(CH_3)_2$] ppm. $C_{29}H_{33}N_2ORh$: calcd. C 65.91, H 6.29, N 5.31; found C 65.41, H, 6.32, 5.41. IR (film from toluene): $\tilde{\nu}$ = 2966, 2918, 2860, 1927 (s), 1464.

Crystal data: CCDC-710644 (for **6**), empirical formula $C_{29}H_{33}N_2ORh$, formula weight 528.48, crystal system triclinic, space group $P\bar{1}$, a = 10.4658(7) Å, b = 11.8571(9) Å, c = 13.2432(8) Å, α = 103.269(3)°, β = 103.291(4)°, γ = 114.368(3)°, V = 1355.87(16) Å, Z = 2, T = 120(2) K, μ = 0.651 mm^{-1}, data collected 26187, unique data 6244, goodness of fit on F^2 = 1.043, $R_{int.}$ = 0.0546, final $R(|F|)$ for $F_o > 2\sigma(F_o)$ = 0.1241, final $R(F^2)$ for all data 0.1286.

Synthesis of Complex 7: Salt (**Ind^{Me}-NHC**)K (0.5 mmol, 220 mg) and $[Ir(COD)Cl]_2$ (0.25 mmol, 176 mg) was dissolved in THF

(20 mL) and combined at –78 °C. CO was bubbled through the solution as it was allowed to reach room temperature. The reaction was stirred for a further 1 h whilst CO was bubbled through. The volatiles were removed under vacuum and the solids re-dissolved in ether and filtered. The resulting crude product was recrystallized from diethyl ether/petroleum ether to give the product as yellow X-ray quality crystals; yield (85%, 274 mg). ^{1}H NMR (C_6D_6, 400 MHz): δ = 7.35 (t, J = 8 Hz, 1 H, Ar), 7.25–7.12 (m, 4 H, Ar), 7.03 (d, J = 5 Hz, 1 H, Ar), 6.41 (d, J = 2 Hz, 1 H, NCH), 6.11 (d, J = 2 Hz, 1 H, NCH), 3.85–3.76 (m, 1 H, bridge), 3.50 (s, 3 H, indenyl-CH_3), 2.95–2.86 [m, 1 H, $CH(CH_3)_2$], 2.90 (s, 3 H, indenyl-CH_3), 2.70–2.60 [m, 1 H, $CH(CH_3)_2$], 1.76 (m, 2 H, bridge), 1.48 [d, J = 7 Hz, 1 H, $CH(CH_3)_2$], 1.38 [d, J = 7 Hz, 1 H, $CH(CH_3)_2$], 1.12 [d, J = 7 Hz, 1 H, $CH(CH_3)_2$], 1.09 [d, J = 7 Hz, 1 H, $CH(CH_3)_2$] ppm. ^{13}C{^{1}H} NMR (C_6D_6, 100 MHz): δ = 145.4 (Ar), 145.0 (Ar), 135.5 (Ar), 135.0 (ArH), 129.7 (ArH), 127.5 (Ar), 126.0 (Ar), 124.3 (Ar), 123.5 (Ar), 123.2 (Ar), 123.0 (ArH), 121.8 (ArH), 120.3 (ArH), 118.7 (ArH), 51.3 (CH_2), 29.3 (CH_2), 27.4 [CH-$(CH_3)_2$], 23.8 (indenyl-methyl), 23.8 (indenyl-methyl), 22.0 [CH-$(CH_3)_2$], 21.7 [$CH(CH_3)_2$], 19.9 [$CH(CH_3)_2$], 17.8 [$CH(CH_3)_2$] ppm. MS (ES$^+$): m/z = 1304 [2M$^+$ + MeCN – CO]. IR (film from benzene): $\tilde{\nu}$ = 2963, 2866, 2023, 1956, 1923, 1657, 1616, 1457, 1411, 1259. $C_{30}H_{33}IrN_2O_2$ (645.82): calcd. C 55.79, H 5.15, N 4.34; found C 55.89, H 5.35, N 4.42.

Crystal data: CCDC-710645 (for **7**), empirical formula $C_{30}H_{33}IrN_2O_2$, formula weight 645.78, crystal system monoclinic, space group $P2_1/c$, a = 8.3743(3) Å, b = 24.0042(16) Å, c = 12.8223(8) Å, α = 90°, β = 90.638(4)°, γ = 90°, V = 2577.4(3) Å^3, Z = 4, T = 120(2) K, μ = 5.210 mm^{-1}, data collected 25444, unique data 5765, goodness of fit on F^2 = 1.069, $R_{int.}$ = 0.0907, final $R(|F|)$ for $F_o > 2\sigma(F_o)$ = 0.0559, final $R(F^2)$ for all data 0.0932.

Catalytic Studies: The catalytic studies were carried out in a stirred autoclave (capacity: approx. 50 cm^3) fitted with a mechanical stirrer (1000 rpm), thermocouple, pressure transducer, bursting disk and injection port. It was linked to a gas ballast vessel through a substrate injection port and a valve capable of controlling the pressure in the autoclave. The autoclave was degassed and filled with the gas to be used [CO for methanol carbonylation, CO/H_2 (1:1) for hydroformylation]. The catalyst solution was injected against a flow of gas into the autoclave, which was then closed and pressurized to 5–10 bar below the required pressure and heated to the desired reaction temperature. Substrate 1-octene (1 cm^3) or methyl acetate (2 cm^3) was then loaded into the injection port. Once the system had stabilized, the substrate was injected into the autoclave using pressure from the ballast vessel and the pressure adjusted to the required reaction pressure, As the reaction proceeded, gas was fed to the autoclave from the ballast vessel to keep the pressure in the autoclave constant. The pressure drop in the ballast vessel was recorded on a computer and used to determine reaction kinetics. The hydroformylation reaction was stopped after 8 h by stopping the stirrer, cooling and venting the autoclave. The liquid phase was analyzed by GCMS [Hewlett–Packard 5890 series gas chromatograph, Supelco™ Meridian MDN-35 low polarity, cross-linked phase comprised of a 35% (phenyl)methylpolysiloxane fused silica capillary column (30m × 0.25mm × 0.25 μm)]. Catalytic solution for methanol carbonylation: **6** (0.026 g, 5×10^{-5} mol) in ethanoic acid (6 cm^3), water (1 cm^3) and iodomethane (1 cm^3), 27 bar.

X-ray Crystallography: A summary of the crystal data, data collection and refinement for compounds **3a**, **3b**, **3c**, **4b**, **5**, **6** and **7** is given above. All data sets except **4b** were collected with a Enraf–Nonius Kappa CCD area detector diffractometer with an FR591 rotating anode (Mo-K_α radiation) and an Oxford Cryosystems low-temperature device operating in ω scanning mode with ψ and ω scans to fill the Ewald sphere. The programs used for control and integration were Collect, Scalepack, and Denzo.[14] The crystals were mounted on a glass fiber with silicon grease, from Fomblin vacuo oil. All solutions and refinements were performed using theWinGX package[15] and all software packages within. Refinements were carried out with all data on F^2 full-matrix least-squares using SHELXL-97.[16] All non-hydrogen atoms were refined using anisotropic thermal parameters, and hydrogen atoms were added using a riding model. There were some difficulties in modelling the structure of **3a** as the electron-density map displayed a large amount of splitting during the modelling process. The NHC ligand was finally modelled as two parts in equal occupancy. The phenyl ring has been modelled as common to both ligand geometries; the angle between the two orientations of the imidazole ring is about 9°. The two positions of fluorenyl ring also lay in much the same position, and have been modelled as being in the same plane. In one orientation, the plane of the imidazol-2-ylidene ring lies only 5.4° from the Rh–$C_{carbene}$ vector whilst in the other orientation it lies as much as 27.7° away. There is also one molecule of THF present in the asymmetric unit which has also been modelled as split into two equal parts. Due to the splitting in the molecule, a number of the bond lengths had to be constrained to give a stable model of the NHC ligand.

Acknowledgments

We thank the University of Southampton for financial support. We are also grateful to Professor W. Clegg at the EPSRC single-crystal synchrotron service at Daresbury[17] for the data collection of complex **4b** and Johnson–Matthey for a loan of rhodium and iridium salts.

[1] a) F. E. Hahn, M. C. Jahnke, *Angew. Chem. Int. Ed.* **2008**, *47*, 4122; b) S. P. Nolan, *N-Heterocyclic Carbenes in Synthesis*, Wiley-VCH, Weinheim **2006**; c) W. A. Herrmann, *Angew. Chem. Int. Ed.* **2002**, *41*, 1290; d) D. Bourisou, O. Guerret, F. P. Gabbai, G. Bertrand, *Chem. Rev.* **2000**, *100*, 39; e) A. T. Normand, K. J. Cavell, *Eur. J. Inorg. Chem.* **2008**, 2781.

[2] A. A. Danopoulos, S. Fiddy, J. Evans, T. Neisius, N. Tsoureas, A. A. D. Tulloch, *Chem. Eur. J.* **2007**, *13*, 3652–3659 and references cited therein.

[3] a) N. D. Clement, L. Routaboul, A. Grotevendt, R. Jackstell, M. Beller, *Chem. Eur. J.* **2008**, *14*, 7408; b) See, for example R. H. Grubbs, *Handbook of Metathesis*, Wiley-VCH, Weinheim, **2006**.

[4] J. M. Praetorius, M. W. Kotyk, J. D. Webb, R. Wang, C. M. Crudden, *Organometallics* **2007**, *26*, 1057 and references cited therein.

[5] A. C. McConnell, P. J. Pogorzelec, A. M. Z. Slawin, G. L. Williams, P. I. P. Elliott, A. Haynes, A. C. Marra, D. J. Cole-Hamilton, *Dalton Trans.* **2006**, 91 and references cited therein.

[6] a) S. P. Downing, A. A. Danopoulos, *Organometallics* **2006**, *25*, 1337; b) A. A. Danopoulos, S. P. Downing, S. Conte-Guadano, D. Pugh, R. Bellabarba, M. Hanton, D. Smith, R. P. Tooze, *Organometallics* **2007**, *26*, 3762; c) B. Wang, D. Wang, D. Cui, W. Gao, T. Tang, X. Chen, X. Jing, *Organometallics* **2007**, *26*, 3167.

[7] A. Pontes da Costa, M. Viciano, M. Sanaú, S. Merino, J. Tejeda, E. Peris, B. Royo, *Organometallics* **2008**, *27*, 1305.

[8] a) A. C. McConnell, P. J. Pogorzelec, A. M. Z. Slawin, G. L. Williams, P. I. P. Elliot, A. Haynes, A. C. Marr, D. J. Cole-Hamilton, *Dalton Trans.* **2006**, 91; b) A. E. C. McConnell, D. F. Foster, P. Pogorzelec, A. M. Z. Slawin, D. J. Law, D. J. Cole-Hamilton, *Dalton Trans.* **2003**, 510; c) D. C. Brookings, S. A. Harrison, R. J. Whitby, B. Crombie, R. V. H. Jones, *Orga-*

nometallics **2001**, *20*, 4574; d) Y. Kataoka, Y. Iwato, T. Yamagata, K. Tani, *Organometallics* **1999**, *18*, 5423.
[9] a) H. M. J. Wang, I. J. B. Lin, *Organometallics* **1998**, *17*, 972; b) A. A. Danopoulos, M. B. Hursthouse, S. Winston, *J. Chem. Soc., Dalton Trans.* **2002**, 3090; c) J. Schutz, W. A. Herrmann, *J. Organomet. Chem.* **2004**, *698*, 2995 and references cited therein.
[10] N. Stylianidis, A. A. Danopoulos, N. T. Tsoureas, *J. Organomet. Chem.* **2005**, *690*, 5948.
[11] a) M. Viciano, M. Sanau, E. Peris, *Organometallics* **2007**, *26*, 6050 and references cited therein; b) M. Poyatos, P. Uriz, J. A. Mata, C. Claver, E. Fernandez, E. Peris, *Organometallics* **2003**, *22*, 440.
[12] a) J. A. Dunn, W. J. Hunks, R. Ruffolo, S. S. Rigby, M. A. Brook, M. J. McGlinchey, *Organometallics* **1999**, *18*, 3372; b) C. S.-W. Lau, W.-T. Wong, *J. Chem. Soc., Dalton Trans.* **1999**, 607.
[13] a) G. Giordano, R. H. Crabtree, *Inorg. Synth.* **1990**, *28*, 88; b) R. Uson, L. A. Oro, J. A. Cabeza, *Inorg. Synth.* **1985**, *23*, 126.
[14] a) R. Hooft, *COLLECT*, Nonius BV, **1997**–2000; b) SCALEPACK, DENZO: Z. Otwinoski, W. Minor, *Methods Enzymol.* **1997**, *276*, 307.
[15] L. J. Farrugia, *J. Appl. Crystallogr.* **1999**, *32*, 83.
[16] G. M. Sheldrick, *Program for Refinement of Crystal Structures*, University of Göttingen, Germany, **1997**.
[17] R. J. Cernik, W. Clegg, C. R. A. Catlow, G. Bushnell-Wye, J. V. Flaherty, G. N. Greaves, M. Hamichi, I. Burrows, D. J. Taylor, S. J. Teat, *J. Synchrotron Radiat.* **1997**, *4*, 279.

Received: November 29, 2008
Published Online: February 27, 2009

